# Wnt Activation After Inhibition Restores Trabecular Meshwork Cells Toward a Normal Phenotype

Kamesh Dhamodaran,[1] Hasna Baidouri,[1] Lyndsey Sandoval,[1] and VijayKrishna Raghunathan[1,2]

[1]Department of Basic Sciences, College of Optometry, University of Houston, Houston, Texas, United States
[2]The Ocular Surface Institute, College of Optometry, University of Houston, Houston, Texas, United States

Correspondence: VijayKrishna Raghunathan, Department of Basic Sciences, College of Optometry, University of Houston, 4901 Calhoun Road, Houston, TX 77204, USA; vraghunathan@uh.edu.

KD and HB contributed equally to the work presented here and should therefore be regarded as equivalent authors.

**Received:** February 10, 2020
**Accepted:** May 14, 2020
**Published:** June 15, 2020

Citation: Dhamodaran K, Baidouri H, Sandoval L, Raghunathan V. Wnt activation after inhibition restores trabecular meshwork cells toward a normal phenotype. *Invest Ophthalmol Vis Sci.* 2020;61(6):30. https://doi.org/10.1167/iovs.61.6.30

**Purpose.** Wnt is a spatiotemporally regulated signaling pathway whose inhibition is associated with glaucoma, elevated intraocular pressure (IOP), and cell stiffening. Whether such changes are permanent or may be reversed is unclear. Here, we determine if activation of Wnt pathway after inhibition reverses the pathologic phenotype.

**Methods.** Primary human trabecular meshwork (hTM) cells from nonglaucomatous donors were cultured for 12 days in the absence or presence of Wnt modulators: (i) LGK974 (*Porcn* inhibitor, 10 µM); (ii) LY2090314 (pGSK3$\beta$ inhibitor, 250 nM); or (iii) 9 days of LGK974 followed by 3 days of LY2090314. Wnt modulation were determined by Western blotting and extracellular matrix (ECM) related genes were evaluated by quantitative PCR. Cytoskeletal morphology was determined by immunofluorescence and cell stiffness by atomic force microscopy.

**Results.** Wnt activation was confirmed by downregulation of pGSK3$\beta$ (0.3-fold; $P < 0.01$), overexpression of *AXIN2* (6.7-fold; $P < 0.001$), and *LEF1* (3.8-fold; $P < 0.001$). Wnt inhibition resulted in dramatic changes in F-actin, which were resolved with subsequent Wnt activation. Concurrently, cell stiffness that was elevated with Wnt inhibition (11.86 kPa; $P < 0.01$) decreased with subsequent Wnt activation (4.195 kPa; $P < 0.01$) accompanied by significant overexpression of phosphorylated YAP (1.8-fold; $P < 0.001$) and TAZ (1.4-fold; $P < 0.001$). Additionally, Wnt activation after inhibition significantly repressed ECM genes (*SPARC* and *CTGF*, $P < 0.01$), cross-linking genes (*LOX* and *TGM2*, $P < 0.05$), inhibitors of matrix metalloproteinases (*TIMP1* and *PAI1*, $P < 0.001$), and overexpressed *MMP 1/9/14* ($P < 0.01$).

**Conclusions.** These data strongly demonstrate that, in normal hTM cells, activation of the Wnt pathway reverses the pathological phenotype caused by Wnt inhibition and may thus be a viable therapeutic for lowering IOP.

Keywords: trabecular meshwork, extracellular matrix, cell mechanics, Wnt pathway, MMPs

Glaucoma, the most common cause of irreversible blindness, are a heterogeneous group of optic neuropathies characterized by retinal ganglion cell loss, retinal nerve fiber layer thinning, and visual field loss.[1] Prevalence of glaucoma is expected to increase from 2.7 million to 6.3 million in the United States between 2010 and 2050.[2] Lowering intraocular pressure (IOP) remains the only modifiable risk factor to impede disease progression. The trabecular meshwork (TM) is considered the primary site for outflow resistance via dynamic interactions between TM cells and their extracellular matrix (ECM) microenvironment. In individuals with POAG the TM is demonstrated to be 20-fold stiffer than those without glaucoma.[3,4] In addition, glaucomatous TM exhibits decreased cellularity,[5] elevated synthesis or deposition of ECM,[6] increased actin contractility,[7] and formation of cross-linked actin networks (CLANs) [8]; this is accompanied by dysregulation of multiple signaling pathways, including but not limited to Wnt/$\beta$-catenin, TGF$\beta$, and bone morphogenetic protein (BMP)[3,7,9–11] pathways. Nevertheless, although crosstalk and feedback between multiple pathways are acknowledged, whether these changes are permanent and/or if they are reversible remains to be investigated.

The Wnt signaling pathway is a highly conserved signal transduction pathway that regulates many cellular functions during development: cell proliferation,[12] cell fate determination,[13] apoptosis,[14] cell polarity, and migration.[15] Wnt/$\beta$-catenin signaling pathways have been studied extensively in numerous ocular diseases like retinal degeneration, cataract, congenital ocular dysfunctions,[16] and glaucoma.[17,18] Wnt inhibitors (e.g. secreted frizzled-related protein 1 [sFRP1][17] and/or Dickkopf-related protein 1 [DKK1]) have been shown to be elevated in glaucoma; overexpression of these proteins is demonstrated to limit aqueous humor (AH) outflow.[19] In previous studies, we showed that sFRP-1 is overexpressed in human trabecular meshwork (hTM) cells cultured on

Table 1. Demographics of Donor Human Corneoscleral Tissues

| hTM | Age/Sex | Experiments Conducted |
|---|---|---|
| 2180 | 68/male | WB, qPCR, F-actin labeling, AFM |
| 74M | 74/male | WB, qPCR, F-actin labeling, AFM |
| 57FOS | 57/female | WB, qPCR, F-actin labeling |
| 2003 | 59/female | WB, F-actin labeling, AFM |

stiffer substrates[20] and Wnt inhibition causes cell stiffening[21]; further, dexamethasone (Dex; a glucocorticosteroid) treatment results in secretion of sFRP1 and DKK1 in the ECM accompanied by ECM stiffening.[9] Independent studies, not related to the Wnt pathway, have shown that the resistance to outflow facility correlates with an increase in TM tissue stiffness.[22] However, it is not known if this pathological phenotype is irreversible and/or subsequently modifiable with intervention.

Recent studies have revealed that pharmacological activation of Wnt signaling plays a major role in various ocular tissues. Wnt activation has been shown to normalize retinal vasculature to help treat familial exudative vitreoretinopathy.[23] Induction of laminin isoforms in human-induced pluripotent stem cell culture promotes their differentiation into neural crest and corneal epithelial cells via Wnt activation.[24] Wnt activation also enhances maintenance of conjunctival epithelial progenitor cells in vitro.[25] Abrogation of stress fibers through Wnt activation was observed in TM cells transfected with wild type myocilin.[26] These studies collectively establish a precedent that Wnt activation may be beneficial to ameliorating the pathology caused by Wnt inhibition in hTM cells. Therefore, we hypothesized that activation of the Wnt pathway subsequent to prolonged Wnt inhibition in primary hTM cells will rescue them toward a healthy phenotype via changes in cell biomechanics, cytoskeletal remodeling, and induction of matrix metalloproteinases (MMPs).

## Materials and Methods

### Isolation and Culture of Primary hTM

Primary hTM cells were isolated from donor corneoscleral rims unsuitable for transplant (SavingSight Eye Bank, St. Louis, MO, USA), as described previously.[27] Donor demographics can be found in Table 1. All experiments were performed in compliance with the tenets of the Declaration of Helsinki. This study is not considered a Human Subject Research, thus is institutional review board (IRB) exempt, because cells were acquired postmortem from de-identified donor tissues. Primary hTM cells were characterized by documenting myocilin response to Dex as recommended (Supplementary Fig. S1).[27] For all experiments, hTM cells were used between passages two and six.

### Wnt Modulation

The hTM cells were routinely cultured in Dulbecco's Modified Eagle Medium : Nutrient Mixture F-12 (DMEM/F12; 1:1) growth media supplemented with 10% fetal bovine serum (FBS; v/v), penicillin/streptomycin. Cells were plated to reach 70 to 80% confluency overnight, following which they were serum deprived by exchanging the growth medium to culture medium containing 0.5% (v/v) FBS for 3 days. Cells were divided into four groups (Fig. 1): (i) *Control:* untreated cells cultured for 12 days in culture media containing 0.5% FBS, with media changes every 3 days; (ii) *Wnt Inhibition:* hTM cells were treated with LGK-974 (10 µM) (Selleckchem, Houston, TX, USA) up to 12 days with (culture) media changes every 3 days. LGK974 is a selective inhibitor of Porcupine *(Porcn)* that blocks the post-translational acylation of Wnt ligands thus inhibiting their secretion.[28] The dose required to inhibit Wnt was based on our prior studies[21]; (iii) *Wnt Activation*: cells were treated with LY2090314 (250 nM) (Selleckchem) up to 12 days with (culture) media changes every 3 days. LY2090314 is an inhibitor of GSK-3$\alpha/\beta$ activity to result in nuclear translocation of $\beta$-catenin and thus activation of the pathway.[29] We empirically determined the nontoxic concentration (0–1 µM) required to inhibit pGSK3ß and activate canonical Wnt signaling while cells were > 80% viable (data not shown); (iv) *Activation after inhibition*: Wnt pathway was first inhibited with LGK974 (10 µM) treatment for 9 days (with two [culture] media changes), following which the pathway was activated by GSK3$\beta$ inhibition (LY2090314; 250 nM) for 3 days. Following the treatment duration, cells were harvested for gene/protein expression, immunocytochemistry, and atomic force microscopy.

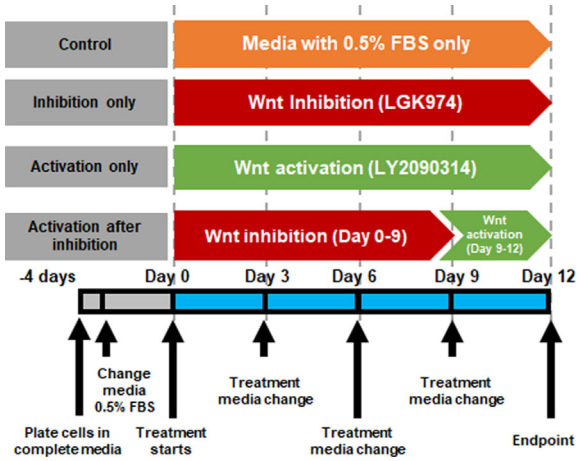


Figure 1. Schematic representation of treatment regimen. The figure illustrates the treatment regimen for in vitro modulation of Wnt signaling in TM cells. Post-treatment, samples were collected for analysis (AFM, gene/protein expression, immunocytochemistry) on day 12.

### Protein Quantitation by Western Blotting

Post-treatment, hTM cells were lysed in radioimmunoprecipitation (RIPA) lysis and extraction buffer (Thermo Scientific, Rockford, IL, USA) with protease/phosphatase inhibitor cocktail (Cell Signaling Technology, Danvers, MA, USA) and quantified using the DC protein assay (Bio-Rad, Hercules, CA, USA). Equal concentration of protein (18 µg) were run on 4 to 15% precast polyacrylamide gels (Bio-Rad) and transferred to polyvinylidene difluoride (PVDF) membranes. Membranes were blocked with 5% bovine serum albumin for 1 hour at room temperature, incubated with respective primary antibodies (Table 2) at 4 deg Celsius (°C) overnight. Membranes were washed and subsequently incubated in species specific secondary antibody for 45 minutes to 1 hour at room temperature. Protein bands were visualized using ECL detection reagents (Western Bright ECL; Advansta, San Jose, CA, USA) and imaged on a ChemiDoc MP (BioRad)

**Table 2.** List of Primary and Secondary Antibodies

| Primary Antibody | Dilution | Vender |
|---|---|---|
| GAPDH (GA1R) | 1: 10000 | Invitrogen, Rockford, IL, USA |
| pGSK3$\beta$ (Tyr216-Tyr279) | 1: 2000 | |
| p$\beta$-Catenin (T41/S45) | 1: 2500 | ABclonal, Woburn, MA, USA |
| RhoA (67B9) | 1: 5000 | Cell Signaling Technology, Danvers, MA, USA |
| CDC42 | 1: 5000 | |
| pYAP(Ser127) (D9W2I) | 1: 2000 | |
| pTAZ (Ser89) (E1X9C) | 1: 5000 | |
| YAP1 | 1: 2500 | Novus Biologicals, Centennial, CO, USA |
| TAZ/WWTR1 | 1: 5000 | |
| **Secondary antibody** | | |
| Peroxidase labeled goat anti-rabbit IgG | 1:10.000 | KPL, Gaithersburg, MD, USA |
| Peroxidase labeled goat anti-mouse IgG | 1:10.000 | |

**Table 3.** List of Primers Used for qPCR

| Gene Name | Sequence (5′-3′) | Size (bp) | Gene Accession |
|---|---|---|---|
| *DKK1* | F: AGCGTTGTTACTGTGGAGAAG R: GTGTGAAGCCTAGAAGAATTACTG | 82 | NM_012242.4 |
| *sFRP1* | F: AGATGCTTAAGTGTGACAAGTTCC R: TCAGATTTCAACTCGTTGTCACAG | 130 | NM_003012.5 |
| *AXIN2* | F: CAGATCCGAGAGGATGAAGAGA R: AGTATCGTCTGCGGGTCTTC | 128 | NM_001363813.1 |
| *LEF1* | F: GACGAGATGATCCCCTTCAA R: CGGGATGATTTCAGACTCGT | 135 | NM_016269.5 |
| *SPARC* | F: GTGCAGAGGAAACCGAAGAG R: AAGTGGCAGGAAGAGTCGAA | 202 | NM_001309444.2 |
| *MYOC* | F: TGTCCGCCAGGTTTTTGAGT R: TGGAAATAGAGGCTCCCCGA | 129 | NM_000261.2 |
| *CTGF* | F: ACCTGTGCCTGCCATTACAA R: GCTTCATGCCATGTCTCCGT | 90 | NM_001901.3 |
| *LOX* | F: CGACCCTTACAACCCCTACA R: AAGTAGCCAGTGCCGTATCC | 117 | NM_002317.7 |
| *TGM2* | F: CTCAGGGCTCACAGTGGAT R: AGGGGTCCTATCTCTCATCCTG | 75 | NM_001323316.1 |
| *MMP1* | F: CCAGGCCCAGGTATTGGAGGGG R: GGCCGAGTTCATGAGCTGCA | 106 | NM_002421.4 |
| *MMP2* | F: ATAACCTGGATGCCGTCGT R: AGGCACCCTTGAAGAAGTAGC | 63 | NM_004530.6 |
| *MMP9* | F: GAACCAATCTCACCGACAGG R: GCCACCCGAGTGTAACCATA | 67 | NM_004994.3 |
| *MMP14* | F: CACCATGAAGGCCATGAGGC R: GTATGTGGCATACTCGCCCA | 175 | NM_004995.4 |
| *TIMP1* | F: ACTACCTGCAGTTTTGTGGCT R: CTGGTCCGTCCACAAGCAA | 162 | NM_003254.3 |
| *PAI1* | F: CCACTTCTTCAGGCTGTTCC R: CCGTTGAAGTAGAGGGCATT | 186 | NM_000602.5 |
| *GAPDH* | F: GGTGAAGGTCGGAGTCAAC R: CCATGGGTGGAATCATATTG | 153 | NM_001289745.3 |

system. Protein band pixel density were quantified using ImageJ Software (https://imagej.nih.gov/ij/).

## Gene Expression by Quantitative Real Time PCR

Post-treatment, hTM cells were lysed and mRNA was extracted using the Purelink RNA mini Kit (Life Technologies, Carlsbad, CA, USA). RNA (1 µg) was converted to cDNA using a high capacity cDNA reverse transcription kit (Applied Biosystems, Foster City, CA, USA). Quantitative real-time PCR was performed on 20 ng of the cDNA with gene specific primers (Table 3) and the PowerUp SYBR Green Master Mix kit (Applied Biosystems) in total volumes of 10 µL per reaction using a CFX Connect Real-time System from Bio-Rad Laboratories (Bio-Rad). The cycle threshold ($C_t$) values obtained from the qPCR equipment and analyzed using the $2^{-\Delta\Delta Ct}$ method with *GAPDH* as the housekeeping gene.

## F-actin Visualization and Immunostaining

Post-treatment, hTM cells were fixed in 4% paraformaldehyde in PBS for 30 minutes at room temperature and further permeabilized/blocked in blocking solution (5% bovine serum albumin, 0.1% Triton X-100 in PBS) for 1 hour at room temperature. Some coverslips (2 coverslips each per cell strain) were incubated Alexa Fluor 594 phalloidin (ThermoFisher Scientific, Eugene, OR, USA) for 20 minutes at room temperature, whereas others (2 coverslips each per cell strain) were incubated with primary antibodies against YAP1 or TAZ (1:250 dilution) at 4°C overnight. This was followed by incubation with species-appropriate secondary antibody conjugated with DyLight 488 (Invitrogen, Rockford, IL, USA) for (1:500 dilution) 1 hour at room temperature. Nuclei were counterstained with 4′,6-diamidino-2-phenylindole (DAPI) (Fisher Scientific, CA, USA) and mounted using mowiol (mowiol is an aqueous mounting medium comprised of polyvinyl alcohol (Mowiol 4-88; Sigma-Aldrich, St. Louis, MO, USA) and glycerol made in 0.2M Tris-Cl buffer (pH 8.5); DABCO (1,4-diazabicyclo-[2,2,2]-octane) was used as antifade). Immunofluorescent images were then captured using an inverted fluorescent microscope (Leica Microsystems AG, Germany) with a ×20 or ×40 objective. For each immunolabelled glass coverslip, 5 to 10 random locations were imaged for all donor strains ($n = 4$). Due to the qualitative nature of imaging, no quantitative measurements were performed at this time. In addition, for each condition per cell strain, the height of 100 cells were determined using $z$-stack. As appropriate, representative images from a single field of view for a single donor are illustrated in the results section(s).

## Cellular Biomechanics by Atomic Force Microscopy

Elastic moduli of cells were determined as described previously.[21,30] Briefly, force-distance curves were obtained in

contact mode using PNP-TR cantilevers (nominal spring constant 0.32 N/m; Nano and More, Watsonville, CA, USA) with a pyramidal tip. For all samples ($n = 4$ donor strains), force curves were obtained from at least 10 cells with 5 force curves for each cell. Elastic modulus was determined using Sneddon model; details of the equation are described elsewhere.[31] Data are represented as violin plots pooling all force curves from each donor strain per treatment.

### Statistical Analysis

Statistical comparison for mechanics, protein, and gene expression among the various groups was done using 1-way ANOVA with Dunnett's multiple post hoc comparisons compared with control cells was used to determine significance. In addition, using *t*-test we compared the results between "Wnt inhibition" and "Wnt activation after inhibition" groups. Results for all comparisons are indicated in the plots and described within the figure legends.

## Results

### Modulation of Wnt Signaling Pathway

The concentration of Wnt inhibitor (LGK974; 10 µM) was based on our previous study.[21] Effective nontoxic concentration of Wnt activator (LY2090314; 250 nm) was determined empirically in a dose-response manner. Wnt inhibition resulted in overexpression of pGSK3$\beta$ (1.44-fold; $P < 0.05$) and p$\beta$-Catenin (1.73-fold; $P < 0.05$) compared with the control group. Consequent to treatment with LY2090314, significant downregulation in pGSK3$\beta$ levels were observed compared with the control group (0.3-fold; $P < 0.01$) (Fig. 2A). *DKK1* and *sFRP1* were used as markers for Wnt antagonism.[19] No significant changes were seen in *DKK1* and *sFRP1* expression after Wnt inhibition, but they remarkably decreased with activation alone (0.37-fold $P < 0.05$, 0.19-fold $P < 0.01$, respectively) or with activation after inhibition (0.3-fold, $P < 0.05$, 0.2-fold, $P < 0.01$, respectively) compared with the untreated control group (Fig. 2B). *AXIN2*[32] and lymphoid enhancer-binding factor 1 (*LEF1*),[33] transcriptional target genes for Wnt, were used as markers of Wnt signaling activation. The mRNA expression of both genes were significantly upregulated with Wnt activation after inhibition (6.7-fold, $P < 0.001$ and 3.7-fold, $P < 0.001$, respectively) and with activation only (6.35-fold, $P < 0.001$ and 3.8-fold $P < 0.001$, respectively) (Fig. 2C). These results collectively demonstrate successful modulation of Wnt signaling in hTM cells.

### Wnt Activation Alters the Cytoskeletal Dynamics

Next, we examined whether Wnt modulated Rho GTPase: RhoA and CDC42 in hTM cells. Rho GTPases regulate cell motility, cytoskeletal dynamics,[34] smooth muscle contractile properties, cell morphology, and trafficking.[35,36] Significant upregulation of RhoA levels after Wnt inhibition (1.6-fold $P < 0.05$) was observed. In contrast, CDC42 were downregulated (0.75-fold, $P < 0.05$) when Wnt was inhibited (Fig. 3). Wnt activation, however, did not appear to modulate RhoA/CDC42 proteins levels when compared with untreated cells. However, in comparison with the Wnt inhibited group, RhoA was suppressed ($P < 0.05$) and CDC42 ($P < 0.05$) was upregulated with Wnt activation following Wnt inhibition. In general, these findings suggest that Wnt activation after inhibition rescues cells from aberrant cytoskeletal protein expression toward a normal phenotype.

### Activation of Wnt Resolves CLAN Like Structures

RhoGTPases are enzymes that regulate the nucleation and formation of filamentous actin (F-actin). Subsequent to changes in RhoA and CDC42, we next determined if there indeed were significant changes in F-actin in hTM cells. Wnt inhibition resulted in the formation of CLAN-like structures compared with presence of stress-fibers only in control samples. These complex geodesic structures were subsequently resolved with Wnt activation (Fig. 4). These data further support the finding that activation of Wnt signaling subsequent to Wnt inhibition may resolve aberrant cytoskeletal remodeling.

### Wnt Activation After Inhibition Reduces Cell Stiffness

Functional consequences to RhoGTPases and F-actin reorganization were evaluated by documenting cell mechanics. As expected and consistent with our previous study,[21] Wnt inhibition increased cellular stiffness compared with control cells (11.86 kPa vs. 4.96 kPa, $P < 0.01$). Cells with Wnt activation alone (3.54 kPa, $P < 0.05$) were significantly softer compared with control cells. Elastic moduli of cells with Wnt activation after inhibition (4.19 kPa) was not significantly different from the control group but was significantly lower compared with Wnt inhibited group ($P < 0.01$) (Fig. 5A). The elastic moduli of cells were obtained over the tallest portion of a cell (i.e. at the location of the nucleus). We were curious if Wnt modulation influenced cell height. We observed that with Wnt activation (either alone or after inhibition) the cell height trended toward an increase, although statistical significance was not achieved (Fig. 5B). We performed Pearson's correlation (Fig. 5C) to determine if a relationship existed between cell height and elastic modulus for each treatment group. We observed significant correlation between the two variables for Wnt inhibition ($P < 0.01$) and Wnt activation after inhibition groups ($P < 0.05$). These findings demonstrate that cellular stiffness was significantly decreased when Wnt was activated even after 9 days of inhibition.

### Wnt Activation Alters the Expression of Hippo Pathway Effectors

We have previously documented that both YAP and TAZ are expressed in hTM cells and may be differentially modulated by substratum stiffness in vitro.[20] Here, we determined if modulation of Wnt signaling was associated with expression and subcellular localization of these proteins. When normalized to total protein levels of YAP1, significant inhibition of phosphorylated YAP1 (pYAP [S127]; $P < 0.05$) was observed with Wnt inhibition (Fig. 6A) accompanied by increased expression of nuclear YAP1 (Fig. 6B) compared with untreated controls. Similarly, Wnt inhibition resulted in greater nuclear accumulation of TAZ (Fig. 6B) although no differences were observed in the ratio of pTAZ to total TAZ. With activation of Wnt, significant increases in ratios of phosphorylated YAP1/TAZ to total YAP1/TAZ, respectively, were observed ($P < 0.001$ for YAP1, and $P < 0.05$ for TAZ; see Fig. 6A) accompanied with more cytosolic retention of these proteins (see Fig. 6B). Overall, the data demonstrates

Investigative Ophthalmology & Visual Science

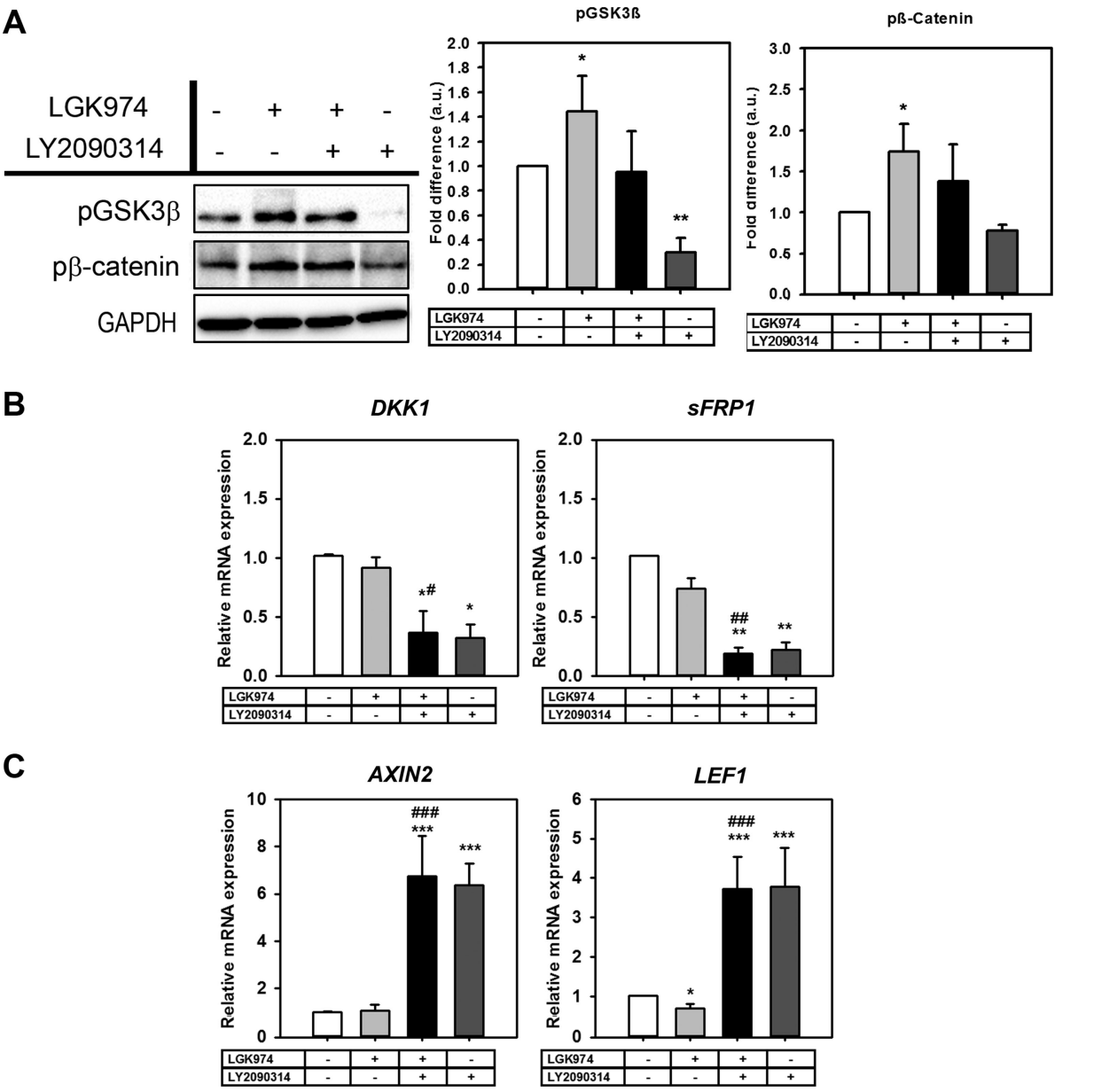


**Figure 2.** LGK974 inhibits while LY2090314 activates Wnt signaling in hTM cells. Primary hTM cells were treated with/without Wnt modulators over 12 days. Whole cell lysates were collected for Western blotting ($n = 4$ donor strains) and gene expression ($n = 3$ donor strains). (**A**) Representative Western blot from a single donor documenting changes in p$\beta$-Catenin (S45/Thr41) and pGSK3$\beta$ protein expression with GAPDH as loading control. Densitometric analysis of blots document a decrease in the p$\beta$-Catenin and pGSK3$\beta$ levels with Wnt activation. (**B**) Wnt activation after 9-days of Wnt inhibition resulted in reduced *DKK1* and *sFRP1* gene expression. (**C**) Relative mRNA expression of *AXIN2* and *LEF1* genes were significantly elevated with Wnt activation regardless of Wnt inhibition. The treatment regimen are as follows: $- - =$ indicates no treatment; $+ - =$ indicates cells were treated with only LGK974; $+ + =$ indicates cells were first treated with LGK974 for 9 days following which they were treated with LY2090314 for 3 days; $- + =$ corresponds to cells treated with only LY2090314. Data presented in histograms are mean $\pm$ standard deviation (SD). Asterisk (*) are used to show comparisons made my 1-way ANOVA followed by Dunnett's post hoc multiple comparison compared with control; $^{*}P < 0.05$; $^{**}P < 0.01$; $^{***}P < 0.001$. Hash symbol (#) denotes Student's *t*-test comparing the results between "Wnt inhibition" and "Wnt activation after inhibition"; $^{\#}P < 0.05$; $^{\#\#}P < 0.01$; $^{\#\#\#}P < 0.001$.

that Wnt activation leads to increased levels of phosphorylation and cytosolic retention of YAP1/TAZ.

## Effects of Wnt Alteration Changes the ECM Expressions

We next investigated whether Wnt modulation influenced ECM expression in hTM cells. The mRNA expression levels of secreted protein acidic and rich in cysteine (SPARC) and connective tissue growth factor (CTGF; downstream target of YAP/TAZ) were significantly downregulated with Wnt activation alone (SPARC: 0.54-fold, $P < 0.05$, CTGF: 0.08-fold, $P < 0.001$) or with Wnt activation after inhibition (0.49-fold, $P < 0.05$, 0.06-fold, $P < 0.001$) (Fig. 7A), whereas Wnt inhibition alone did not affect expression of these genes. On the other hand, where Wnt inhibition overexpressed ECM cross-linking genes (LOX: 1.35-fold; TGM2: 2.1-fold, $P < 0.05$),

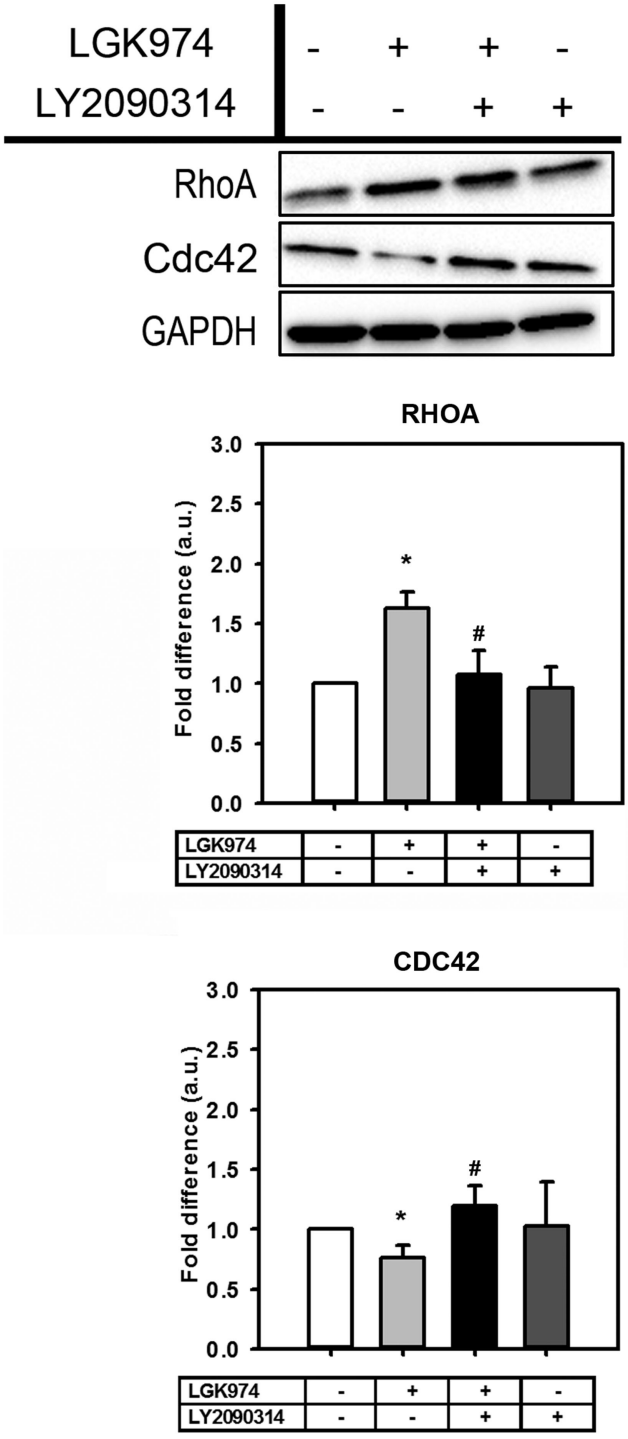


**Figure 3.** Wnt modulation alters RhoGTPases that regulate cytoskeletal dynamics. Representative Western blot from a single donor documenting changes in expression levels of RhoA and CDC42 protein expression ($n = 4$ donor strains). The treatment regimen are as follows: $- -$ = indicates no treatment; $+ -$ = indicates cells were treated with only LGK974; $+ +$ = indicates cells were first treated with LGK974 for 9 days following which they were treated with LY2090314 for 3 days; $- +$ = corresponds to cells treated with only LY2090314. Densitometric analysis of blots are illustrated as histograms as mean ± standard deviation (SD). Asterisk (*) are used to show comparisons made my 1-way ANOVA followed by Dunnett's post hoc multiple comparison compared with control; $^{*}P < 0.05$; $^{**}P < 0.01$, $^{***}P < 0.001$. Hash symbol (#) denotes Student's *t*-test comparing results between "Wnt inhibition" and "Wnt activation after inhibition"; $^{\#}P < 0.05$; $^{\#\#}P < 0.01$; $^{\#\#\#}P < 0.001$.

Wnt activation significantly reduced their expression either by itself (LOX: 0.32-fold, $P < 0.01$; TGM2: 0.44-fold, $P < 0.05$) or when activated after Wnt inhibition (LOX: 0.19-fold, $P < 0.001$; *TGM2:* 1.0-fold, $P < 0.05$) (Fig. 7B).

Next, we investigated changes in genes involved in ECM turnover. Wnt modulation did not significantly alter *MMP2* expression. Where Wnt inhibition downregulated MMP1 (0.09-fold, $P < 0.001$), its expression was upregulated when Wnt was activated alone (2.83-fold, $P < 0.05$) or when activated following Wnt inhibition (2.58-fold, $P < 0.001$). Similarly, MMP9 and MMP14 were all upregulated with Wnt activation either by itself (13.68-fold, $P < 0.05$, or 5.37-fold, $P < 0.001$, respectively) or when activated after Wnt inhibition (9.15-fold, $P < 0.01$, or 5.02-fold, $P < 0.001$, respectively).

Concurrently, inhibitor of metalloproteinase 1 (TIMP1) was upregulated with Wnt inhibition (1.9-fold, $P < 0.05$), but was significantly downregulated when Wnt was activated alone (0.30-fold, $P < 0.001$) or when activated following Wnt inhibition (0.5-fold, $P < 0.001$) (Fig. 7C). Plasminogen activator inhibitor-1 (PAI-1), a serine protease inhibitor, was also downregulated after Wnt activation alone (0.33-fold, $P < 0.001$), or activation following Wnt inhibition (0.34-fold, $P < 0.001$).

### Effects of Wnt Modulators Change in Myocilin Expressions

Myocilin (MYOC), a matricellular protein abundantly expressed in glaucomatous TM,[37] was significantly altered both at gene and protein levels. Gene expression was reduced with Wnt activation (0.24-fold, $P < 0.01$) alone or with activation after inhibition (0.22-fold, $P < 0.01$) compared to the control group (Fig. 8A). Although gene expression trended to be overexpressed with Wnt inhibition, due to large donor-to-donor variability, statistical significance was not achieved. However, the MYOC protein level was significantly upregulated (2.12-fold, $P < 0.01$) with Wnt inhibition (Fig. 8B) while being reduced with Wnt activation (0.23-fold, $P < 0.01$) alone or with activation after inhibition (0.46–fold, $P < 0.01$) compared to the control group.

## Discussion

POAG is the most common type of glaucoma leading to irreversible vision loss with IOP as the only modifiable risk factor. The TM is considered a major regulator of aqueous humor outflow facility to maintain normal levels of IOP. Damage to cells in the TM is correlated with ocular hypertension and progression of glaucoma. Secreted factors (such as cytokines and growth factors) concurrent with changes in gene/protein expression in TM cells orchestrate the remodeling of ECM, and together these have been associated with POAG.[38] The molecular mechanisms underlying the etiology and progression of TM pathology, however, remains unclear. Among the many pathways suggested to be dysregulated in disease, the Wnt signaling pathway is one that is strongly implicated in glaucomatous TM.[19,21] This pathway is conserved, critical during development, and regulates cell fate during embryogenesis; but is also implicated in playing a crucial role in tissue homeostasis.[39] We have previously demonstrated that chronic treatment of normal TM cells with Dex results in the increased secretion of Wnt inhibitors (DKK1 and sFRP1) into the ECM in vitro.[9] Overexpressing Wnt antagonists, sFRP1 and DKK1, in mice can result in

Investigative Ophthalmology & Visual Science

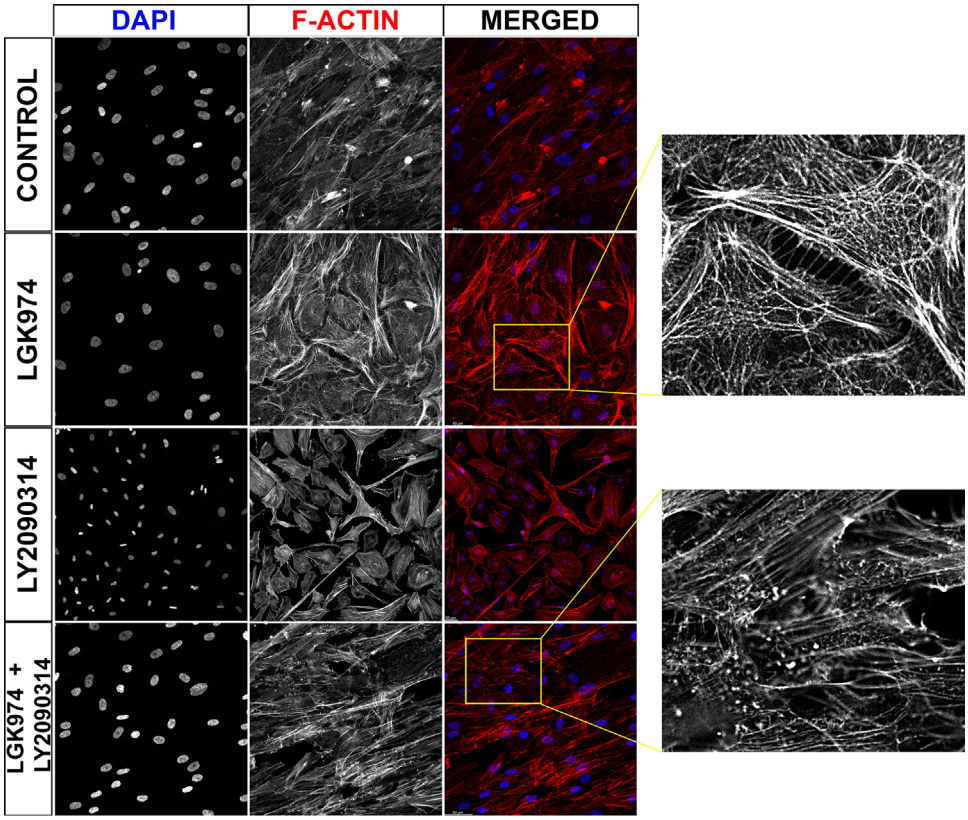


**Figure 4.** Activation of Wnt pathway resolves CLAN-like structures. Primary hTM cells ($n = 4$ donor strains) cultured on glass coverslips were treated with/without Wnt signal modulators for 12 days following which cells were fixed and stained with Phalloidin to visualize F-actin. There were 10 random fields per coverslip per donor strain that were imaged. Representative image demonstrates F-actin (*red*), and nuclei (*blue*) labeling respectively. Insets demonstrate alterations in actin cytoskeleton in gray scale. Scale bar indicates 50 µm.

elevated IOP, reduced outflow facility, and degeneration of TM tissues.[17,19] In this study, through inhibition of *Porcn* using LGK974, we do not observe any significant changes in gene expression for *sFRP1/DKK1*. This is likely due to a reduction in secretion of Wnt ligands, mediated by suppression of *Porcn'* acyltransferase activity, leading to a disruption in an important feedback loop. Nevertheless, as expected, an upregulation in phosphorylated $\beta$-catenin accompanied with increased phosphorylation of GSK3$\beta$ demonstrates Wnt inhibition.[39–41] Inhibition of pGSK3$\beta$, with LY2090314, and subsequent activation of canonical Wnt/$\beta$-catenin signaling was confirmed through overexpression of *AXIN2*[42] and *LEF1*[33] regardless of prior Wnt inhibition; this was accompanied by significant repression of Wnt inhibitors, *sFRP1* and *DKK1*. This is important when we consider our findings from a prior study[21] where cells remained in a disruptive state, despite removal of Wnt inhibitor, prolonging a pathologic phenotype. Thus, our approach of activating Wnt after Wnt inhibition may break this cycle and facilitate reversal of TM cells toward normalcy.

## Wnt Modulation Alters Cytoskeletal Dynamics, Mechanotransduction, and Cellular Biomechanics

RhoGTPases are an important effector of the noncanonical Wnt planar cell polarity (PCP) pathway.[43] The PCP signaling plays a key mediator in orchestrating cell, tissue organization, and its function are mediated via changes in the actin cytoskeleton. Our data demonstrates that overexpression of RhoA caused by Wnt inhibition can be reversed by subsequent Wnt activation. This is consistent with previous studies that document RhoA inactivation through the activation of canonical Wnt/$\beta$-catenin signaling in the murine cancer cells.[44,45] Activation of RhoGTPases are also associated with nucleation of F-actin which may adversely stiffen cells. Consistent with our previous study,[21] here, we demonstrated that Wnt inhibition results in significant cell stiffening, which is reversed with subsequent Wnt activation. In fact, cells were slightly yet significantly softer with Wnt activation than untreated or Wnt inhibited cells. Noncanonical Wnt activation has been demonstrated to induce CLAN formation, which is reversible with Ror2 knockdown.[46] Currently though, there is no causal link to establish that CLANs are profibrotic, compared with nonglaucomatous TM cells glaucomatous TM cells present with an increase in CLANs.[47–49] In addition, steroid and TGF$\beta$2 treatment of TM cells induce CLAN formation[50–52]; both steroid and TGF$\beta$2 have been associated with elevations in IOP, increased actin contractility and Rho kinase activity. In addition, $\beta$1 and $\beta$3 integrins have been shown to enhance CLAN formation.[53] Induction of CLANs have been associated with reduced TM proliferation, migration, and phagocytosis[54–56]; features that have been attributed as a profibrotic dysfunction of the TM. Although we specifically did not count the number of cells that form CLANs, here, we observed dramatic changes in F-actin organization, with Wnt inhibition, resembling CLAN-like geodesic structures that has been speculated

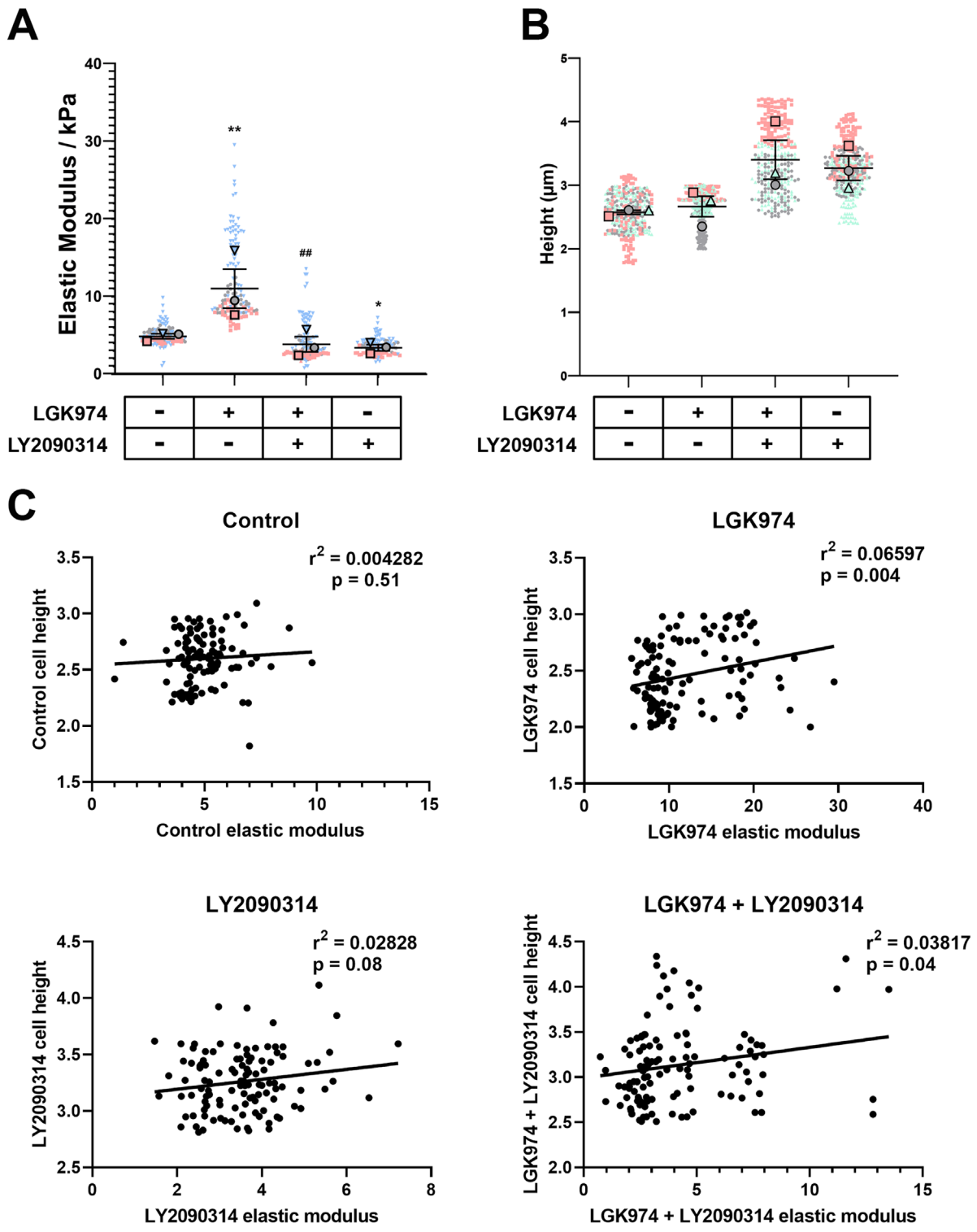


**Figure 5.** Activation of Wnt softens hTM cells. (**A**) Primary hTM cells were cultured in FluoroDish tissue culture dishes with/without Wnt modulators for 12 days. Cell mechanics were determined by atomic force microscopy. Data are represented as violin plots with mean ± standard error in mean (SEM) indicated in the plot. Results are data pooled from all force curves obtained from the four donor strains. (**B**) The height of hTM cells in the various treatment groups was calculated from the highest point of the cell above the nucleus to the underlying substratum. Results are from at least 100 cells per treatment group for each donor strain. Data are represented with individual data points as dots overlaid with mean ± standard error in mean (SEM) from $n = 3$ biological donor strains. The treatment regimen are as follows: − − = indicates no treatment; + − = indicates cells were treated with only LGK974; + + = indicates cells were first treated with LGK974 for 9 days following which they were treated with LY2090314 for 3 days; − + = corresponds to cells treated with only LY2090314. Asterisk (*) are used to show comparisons made my 1-way ANOVA followed by Dunnett's post hoc multiple comparison compared with control; $^{*}P < 0.05$; $^{**}P < 0.01$. Hash symbol (#) denotes Student's *t*-test comparing results between "Wnt inhibition" and "Wnt activation after inhibition"; $^{\#\#}P < 0.01$. (**C**) Pearson's correlation to demonstrate relationship between elastic moduli of cells versus cell height. Data were pooled from all four donor strains for each treatment.

Investigative Ophthalmology & Visual Science

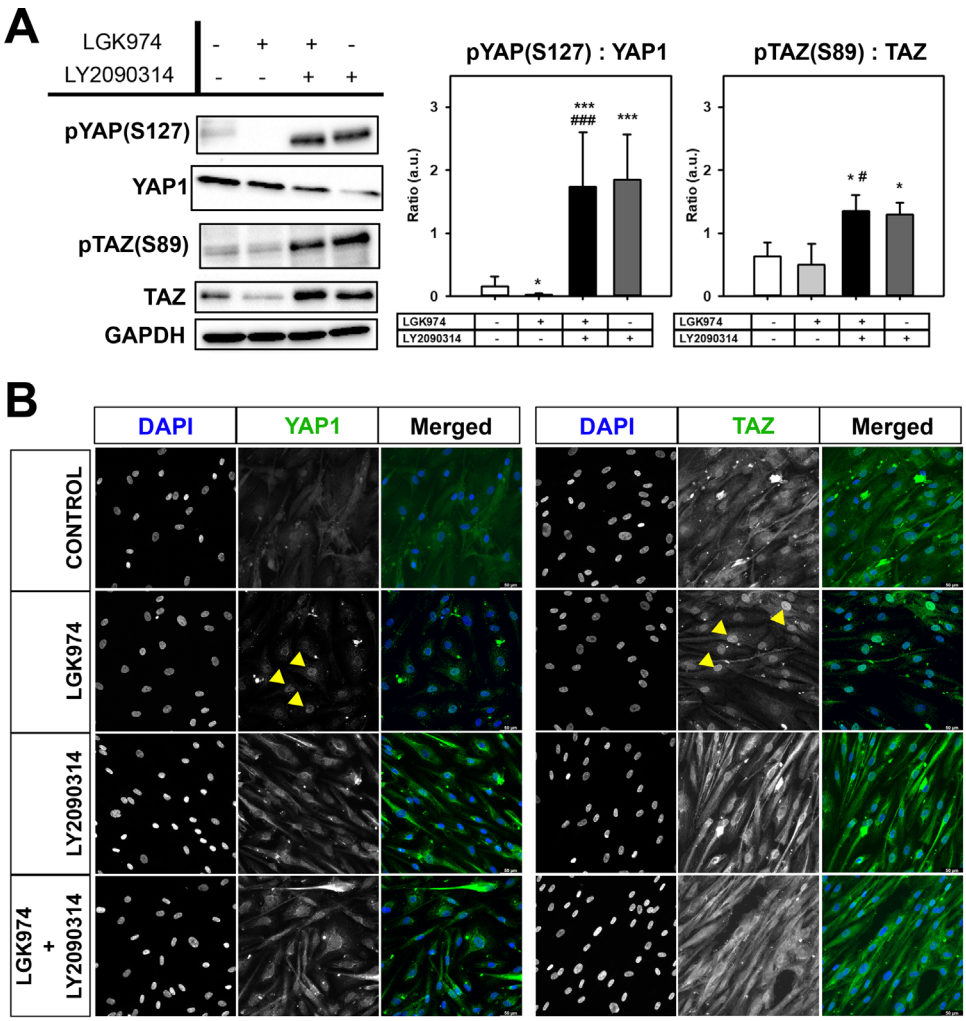


**Figure 6.** Wnt modulation affects YAP/TAZ phosphorylation and localization. (**A**) Representative Western blot analysis ($n = 3$ donor strains) demonstrating the effects of Wnt modulation on the ratio of phosphorylated protein levels to total protein levels for the hippo pathway effectors YAP1/TAZ. Wnt activation regardless of Wnt inhibition significantly increased their cellular phosphorylation levels. Histograms show average of relative levels of pYAP1:YAP1 or pTAZ:TAZ corrected for GAPDH levels. (**B**) Representative image demonstrating the subcellular localization of YAP1 or TAZ (*green*) and nuclei (*blue*) in cells across the treatment groups. *Yellow arrows* indicate localization of YAP1 or TAZ in the nucleus after Wnt inhibition. The treatment regimen are as follows: − − = indicates no treatment; + − = indicates cells were treated with only LGK974; + + = indicates cells were first treated with LGK974 for 9 days following which they were treated with LY2090314 for 3 days; − + = corresponds to cells treated with only LY2090314. Asterisks (*) are used to show comparisons made my 1-way ANOVA followed by Dunnett's post hoc multiple comparison compared with control; $^{*}P < 0.05$; $^{**}P < 0.01$; $^{***}P < 0.001$. Hash symbol (#) denotes Student's *t*-test comparing results between "Wnt inhibition" and "Wnt activation after inhibition"; $^{\#}P < 0.05$; $^{\#\#}P < 0.01$; $^{\#\#\#}P < 0.001$.

to be associated with stiffer cells.[54] Whereas Mao et al. demonstrated that activation of canonical Wnt via Wnt3A had no influence on CLAN formation,[19] Webber et al.[57] demonstrated that Wnt3a, increased K-cadherin expression to reduce transcellular resistance and ocular hypertension. Our data show that Wnt activation via inhibition of pGSK3$\beta$ was enough to resolve the complex CLAN-like reorganization. We thus speculate that the method used to activate canonical Wnt signaling may be important and may result in different downstream targets being differentially modulated. Further studies are required to validate this hypothesis, and to definitively tie CLANs with TM pathology and biomechanical changes. However, relaxation of the actin cytoskeleton is thought to decrease cellular contractility, and increase AH outflow,[58] thus supporting our result that Wnt activation may be beneficial to restoring TM cell function. Wnt inhibition also resulted in inhibition of CDC42 here, which can adversely impact proliferation, polarity, migration, and differentiation of cells disrupting homeostasis.[59] In addition, suppression of CDC42 is thought to disrupt formation of tunneling nanotubes (TNTs)[60] that are essential for intercellular communication in TM culture.[61] Again, activation of Wnt was able to rescue CDC42 suppression in TM cells.

RhoGTPases are thought to regulate signal transduction via mechanotransducers and transcriptional coactivators of the Hippo pathway, YAP, and TAZ.[62,63] Dupont et al.[64] demonstrated that transcriptional activity of YAP/TAZ requires Rho activation and tension in the cytoskeleton. In line with this, Wnt inhibition resulted in a decrease in the phosphorylation of YAP at S127 and TAZ at S89 triggering its nuclear localization. Nuclear YAP/TAZ can constitutively trigger overexpression of ECM crosslink-

Investigative Ophthalmology & Visual Science

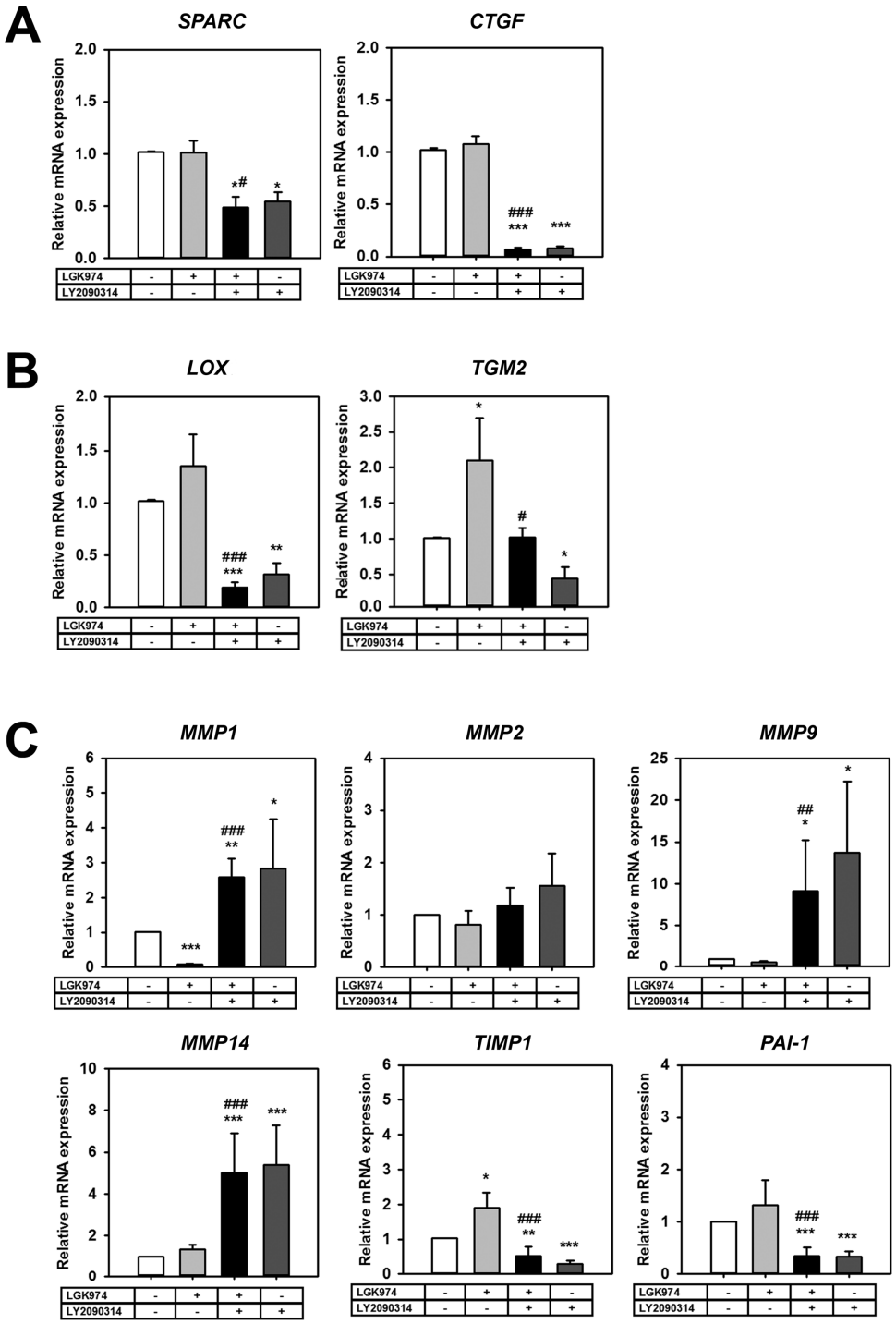


**Figure 7.** Wnt modulation alters expression of ECM regulating genes. Primary hTM cells ($n = 3$ donor strains) were cultured with/without Wnt signal modulators for 12 days following which mRNA was isolated and qPCR was performed. (**A**) Matricellular genes *SPARC* and *CTGF* were significantly downregulated with Wnt activation. (**B**) ECM cross-linking genes (*LOX*, and *TGM2*) were elevated with Wnt inhibition and significantly inhibited with subsequent Wnt activation. (**C**) ECM turnover proteins *MMPs1*, *9*, and *14* were upregulated with Wnt activation but repressed with Wnt inhibition. Likewise, inhibitors of MMPs (*TIMP1* and *PAI-1*) were remarkably reduced with Wnt activation. The treatment regimen are as follows: − − = indicates no treatment; + − = indicates cells were treated with only LGK974; + + = indicates cells were first treated with LGK974 for 9 days following which they were treated with LY2090314 for 3 days; − + = corresponds to cells treated with only LY2090314. Asterisks (*) are used to show comparisons made my 1-way ANOVA followed by Dunnett's post hoc multiple comparison compared with control; $^{*}P < 0.05$; $^{**}P < 0.01$; $^{***}P < 0.001$. Hash symbol (#) denotes Student's *t*-test comparing results between "Wnt inhibition" and "Wnt activation after inhibition"; $^{\#}P < 0.05$; $^{\#\#}P < 0.01$;, $^{\#\#\#}P < 0.001$.

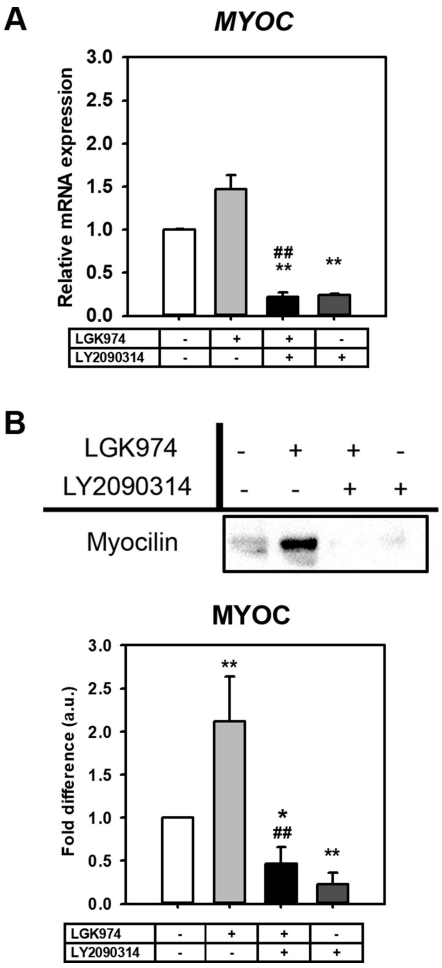


**Figure 8.** Wnt modulation significantly alters MYOC expression. Myocilin expression with Wnt modulation was documented by (**A**) qPCR ($n = 3$ donor strains), and (**B**) Western blotting ($n = 4$ donor strains). Both mRNA and proteins levels of MYOC were drastically reduced with Wnt activation. However, increases in *MYOC* expression after Wnt inhibition were statistically significant only at the protein level. The treatment regimen are as follows: $- - =$ indicates no treatment; $+ - =$ indicates cells were treated with only LGK974; $+ + =$ indicates cells were first treated with LGK974 for 9 days following which they were treated with LY2090314 for 3 days; $- + =$ corresponds to cells treated with only LY2090314. Asterisks (*) are used to show comparisons made my 1-way ANOVA followed by Dunnett's post hoc multiple comparison compared with control; $^{*}P < 0.05$; $^{**}P < 0.01$; $^{***}P < 0.001$. Hash symbol (#) denotes Student's *t*-test comparing results between "Wnt inhibition" and "Wnt activation after inhibition"; $^{\#}P < 0.05$; $^{\#\#}P < 0.01$; $^{\#\#\#}P < 0.001$.

ers (TGM2 and LOX),[64–66] and connective tissue growth factor (CTGF) and TGF$\beta$, two growth factors that have been associated with glaucoma.[67–70] Subsequent activation of canonical Wnt resulted in corresponding increases in pYAP(S127)/pYAZ(S89) and their cytoplasmic retention suggesting a resultant inhibition of their transcriptional function. Curiously, cytoplasmic YAP/TAZ, widely documented in cells cultured on softer substrates,[64] is reflective of softer cells considering cells cultured on softer substrates are intrinsically softer.[71,72] Collectively, our data demonstrate that activation of Wnt decreases RhoA, restores CDC42, resolves complex F-actin reorganization, softens cells, and is associated with cytoplasmic YAP/TAZ.

## Wnt Modulation Dynamically Alters Extracellular Matrix Regulatory Gene Expression

Because one of the major effects of Wnt inhibition is an increase in resistance to AH outflow, we next explored if activating Wnt after its inhibition beneficially modulates genes that regulate the ECM. Here, we document that Wnt inhibition upregulated the expressions of multiple ECM genes (*SPARC*, *CTGF*, and *MYOC*) and ECM crosslinkers (*TGM2* and *LOX*) while simultaneously inhibiting expression of MMPs (*MMP1* and *MMP9*). Interestingly, *CTGF*, *TGM2*, *LOX*, and *PAI-1* are all downstream transcriptional targets of YAP/TAZ.[64–66] SPARC is a multifunction protein that modulates cell shape, adhesion, interactions with the ECM,[73] and affects the expression of MMPs and some growth factors.[74] In fact, overexpression of SPARC increased IOP via alterations in the ECM.[75] Similarly, chronic upregulation of CTGF leads to cellular stress, increase in TM ECM actin-mediated contractility[76] and ocular hypertension in mice.[69] Mutations in myocilin have been associated with POAG, cause endoplasmic reticular stress and elevate IOP.[77–80]

Biomechanical properties of the ECM depend not only on composition, but also on organization and post-translational modifications, such as crosslinking.[81] The LOX family proteins catalyze the crosslinking of collagens and elastin through oxidative deamination of lysine and hydroxylysine residues, which stabilize collagen and elastin fibers in the ECM.[82,83] Transglutaminase enzymes catalyze the post-translational modification of proteins through the formation of isopeptide bonds resulting in crosslinking of ECM proteins, including fibronectin, collagen, laminin, and elastin.[84–86] Thus, crosslinking of ECM proteins prevents proteolytic breakdown and results in decreased ECM turnover, ECM accumulation, and tissue stiffness.[87] Overexpression of tissue transglutaminase 2 (TGM2) has been shown to elevate IOP in mice.[88,89] Keller et al. demonstrated that ECM turnover initiated by MMPs in the TM were necessary to maintain the outflow facility and homeostasis.[90,91] Altogether, Wnt inhibition resulted in deleterious effects on ECM regulatory genes. Activation of canonical Wnt signaling, irrespective of whether Wnt inhibition was present, reversed the above observed changes. We saw potent elevation in *MMPs*, downregulation of *CTGF*, *SPARC*, *MYOC*, *LOX*, and *TGM2* accompanied by significant downregulation of inhibitors of *MMPs*, such as *TIMP1* and *PAI-1*. These suggest that the ability of cells to restore ECM homeostasis may not be irreversibly damaged; thus, intervention to restore outflow facility may be effective.

## Limitations

Although the results presented here are consistent with each other, this study is not without limitations. First, all of our experiments were performed in vitro to identify molecular changes in the signaling pathway. Thus, extrapolations of our data to what may be observed in vivo, or ex vivo should be done so cautiously considering functional changes in outflow resistance and facility were not determined. Second, we use small molecule compounds to modulate Wnt signaling. Whereas such use has numerous advantages, their effects are dose-time dependent, and, thus, may inflict off-target effects when used for longer periods of time. This is especially true because the Wnt pathways intersects with numerous other signaling pathways. Additional studies using a genetic approach with targeted gene

Investigative Ophthalmology & Visual Science

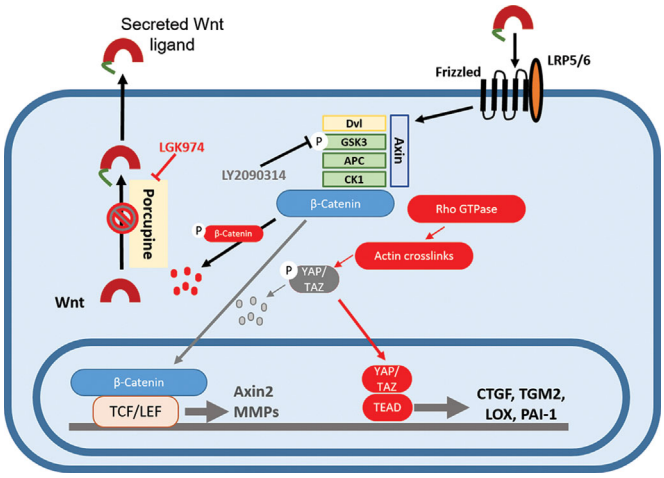


**Figure 9.** Schematic summary of the effect of Wnt modulation on TM cells. TM cells were treated with LGK974 to inhibit *Porcn* in the endoplasmic reticulum (ER) to block post-translational acylation of Wnt ligands, thus restricting their secretion. This results in the increased formation of CLAN-like structures, elevated cell stiffness, transcriptional activation of YAP/TAZ to overexpress *TGM2*, *CTGF*, *LOX*, and suppress *MMPs*. Subsequently, treatment of TM cells with GSK3$\beta$ inhibitor, LY2090314, results in nuclear translocation of $\beta$-catenin to activate its transcription. This results in the elevated expression of downstream target genes like *AXIN2*, *LEF1*, and *MMPs* accompanied by cytoplasmic retention of YAP/TAZ and reduced expression of *CTGF*, *TGM2*, *LOX*, and *PAI-1*, resolution of adverse actin remodeling and softening of TM cells.

silencing/knock-in/mutations may be essential to dissect a causal relationship between the Wnt and YAP/TAZ pathways. Finally, all of our in vitro studies were performed on glass/tissue culture plastic whose mechanical and chemical properties are far removed from the native microenvironment that cells perceive in vivo. Thus, future investigations will be required by culturing cells on hydrogels of varying stiffness or on cell derived matrices/engineered scaffolds mimicking the properties of the native TM.

## Conclusion

In summary (Fig. 9), we demonstrate here that perturbing secretion of Wnt ligands by targeting *Porcn* results in triggering pathology in TM cells in the form of cytoskeletal remodeling, cell stiffness, overexpression of ECM genes, upregulation of ECM crosslinkers, and decreases in MMPs with simultaneous overexpression of inhibitors of MMPs; these changes may partially be due to translocation of YAP/TAZ to the nucleus. Subsequently, we demonstrate that this pathologic phenotype is reversible with canonical Wnt activation via inhibition of pGSK3$\beta$. Specifically, this resulted in cell softening, resolution of CLAN-like structures, cytoplasmic retention of YAP/TAZ, decreased expression of ECM crosslinkers, and inhibitors of MMPs with upregulation of specific MMPs responsible for ECM turnover. We thus speculate that GSK3$\beta$ may be potent molecular target for the reduction of IOP.

## *Acknowledgments*

The authors thank their funding sources. We would also like to thank SavingSight (Kansas City, MO) eye bank for procuring all human donor eyes used in this work. Most importantly, we would like to thank the families of the organ donors without whose consent these experiments would be impossible.

Supported by startup funding from UHCO (VKR), NIH/National Eye Institute (NEI) Grants EY026048-01A1 (VKR), and NIH-T35 Training Grant EY007088 (LS).

Disclosure: **K. Dhamodaran**, None; **H. Baidouri**, None; **L. Sandoval**, None; **V. Raghunathan**, None

## *References*

1. Allingham RR, Liu Y, Rhee DJ. The genetics of primary open-angle glaucoma: a review. *Exp Eye Res*. 2009;88:837–844.
2. National Institutes of Health/National Eye Institute (NIH.NEI). Glaucoma data and statistics - Projections for glaucoma (2010-2030-2050). Available at: https://www.nei.nih.gov/learn-about-eye-health/resources-for-health-educators/eye-health-data-and-statistics/glaucoma-data-and-statistics 2019.
3. Last JA, Pan T, Ding Y, et al. Elastic modulus determination of normal and glaucomatous human trabecular meshwork. *Invest Ophthalmol Vis Sci*. 2011;52:2147–2152.
4. Vahabikashi A, Gelman A, Dong B, et al. Increased stiffness and flow resistance of the inner wall of Schlemm's canal in glaucomatous human eyes. *Proc Natl Acad Sci U S A*. 2019;116:26555–26563.
5. Alvarado J, Murphy C, Juster R. Trabecular meshwork cellularity in primary open-angle glaucoma and nonglaucomatous normals. *Ophthalmology*. 1984;91:564–579.
6. Vranka JA, Kelley MJ, Acott TS, Keller KE. Extracellular matrix in the trabecular meshwork: intraocular pressure regulation and dysregulation in glaucoma. *Exp Eye Res*. 2015;133:112–125.
7. Clark AF, Miggans ST, Wilson K, Browde S, McCartney MD. Cytoskeletal changes in cultured human glaucoma trabecular meshwork cells. *J Glaucoma*. 1995;4:183–188.
8. Job R, Raja V, Grierson I, et al. Cross-linked actin networks (CLANs) are present in lamina cribrosa cells. *Br J Ophthalmol*. 2010;94:1388–1392.
9. Raghunathan VK, Morgan JT, Park SA, et al. Dexamethasone stiffens trabecular meshwork, trabecular meshwork cells, and matrix. *Invest Ophthalmol Vis Sci*. 2015;56:4447–4459.

10. Grierson I, Howes RC. Age-related depletion of the cell population in the human trabecular meshwork. *Eye (Lond)*. 1987;1(Pt 2):204–210.
11. Wordinger RJ, Fleenor DL, Hellberg PE, et al. Effects of TGF-beta2, BMP-4, and gremlin in the trabecular meshwork: implications for glaucoma. *Invest Ophthalmol Vis Sci*. 2007;48:1191–1200.
12. Nayak G, Odaka Y, Prasad V, et al. Developmental vascular regression is regulated by a Wnt/beta-catenin, MYC and CDKN1A pathway that controls cell proliferation and cell death. *Development*. 2018;145:dev154898.
13. Rajakulendran N, Rowland KJ, Selvadurai HJ, et al. Wnt and Notch signaling govern self-renewal and differentiation in a subset of human glioblastoma stem cells. *Genes Dev*. 2019;33:498–510.
14. Pecina-Slaus N. Wnt signal transduction pathway and apoptosis: a review. *Cancer Cell Int*. 2010;10:22.
15. Ng LF, Kaur P, Bunnag N, et al. WNT signaling in disease. *Cells*. 2019;8:826.
16. de Iongh RU, Abud HE, Hime GR. WNT/Frizzled signaling in eye development and disease. *Front Biosci*. 2006;11:2442–2464.
17. Wang WH, McNatt LG, Pang IH, et al. Increased expression of the WNT antagonist sFRP-1 in glaucoma elevates intraocular pressure. *J Clin Invest*. 2008;118:1056–1064.
18. Webber HC, Bermudez JY, Sethi A, Clark AF, Mao W. Crosstalk between TGFbeta and Wnt signaling pathways in the human trabecular meshwork. *Exp Eye Res*. 2016;148:97–102.
19. Mao W, Millar JC, Wang WH, et al. Existence of the canonical Wnt signaling pathway in the human trabecular meshwork. *Invest Ophthalmol Vis Sci*. 2012;53:7043–7051.
20. Raghunathan VK, Morgan JT, Dreier B, et al. Role of substratum stiffness in modulating genes associated with extracellular matrix and mechanotransducers YAP and TAZ. *Invest Ophthalmol Vis Sci*. 2013;54:378–386.
21. Morgan JT, Raghunathan VK, Chang YR, Murphy CJ, Russell P. Wnt inhibition induces persistent increases in intrinsic stiffness of human trabecular meshwork cells. *Exp Eye Res*. 2015;132:174–178.
22. Wang K, Li G, Read AT, et al. The relationship between outflow resistance and trabecular meshwork stiffness in mice. *Sci Rep*. 2018;8:5848.
23. Wang Z, Liu CH, Sun Y, et al. Pharmacologic activation of Wnt signaling by lithium normalizes retinal vasculature in a murine model of familial exudative vitreoretinopathy. *Am J Pathol*. 2016;186:2588–2600.
24. Shibata S, Hayashi R, Okubo T, et al. Selective laminin-directed differentiation of human induced pluripotent stem cells into distinct ocular lineages. *Cell Rep*. 2018;25:1668–1679, e1665.
25. Schrader S, O'Callaghan AR, Tuft SJ, Beaconsfield M, Geerling G, Daniels JT. Wnt signalling in an in vitro niche model for conjunctival progenitor cells. *J Tissue Eng Regen Med*. 2014;8:969–977.
26. Shen X, Ying H, Yue BY. Wnt activation by wild type and mutant myocilin in cultured human trabecular meshwork cells. *PLoS One*. 2012;7:e44902.
27. Keller KE, Bhattacharya SK, Borras T, et al. Consensus recommendations for trabecular meshwork cell isolation, characterization and culture. *Exp Eye Res*. 2018;171:164–173.
28. Liu J, Pan S, Hsieh MH, et al. Targeting Wnt-driven cancer through the inhibition of Porcupine by LGK974. *Proc Natl Acad Sci U S A*. 2013;110:20224–20229.
29. Atkinson JM, Rank KB, Zeng Y, et al. Activating the Wnt/beta-catenin pathway for the treatment of melanoma–application of LY2090314, a novel selective inhibitor of glycogen synthase kinase-3. *PLoS One*. 2015;10:e0125028.
30. Chang YR, Raghunathan VK, Garland SP, Morgan JT, Russell P, Murphy CJ. Automated AFM force curve analysis for determining elastic modulus of biomaterials and biological samples. *J Mech Behav Biomed Mater*. 2014;37:209–218.
31. McKee CT, Last JA, Russell P, Murphy CJ. Indentation versus tensile measurements of Young's modulus for soft biological tissues. *Tissue Eng Part B Rev*. 2011;17:155–164.
32. Lustig B, Jerchow B, Sachs M, et al. Negative feedback loop of Wnt signaling through upregulation of conductin/axin2 in colorectal and liver tumors. *Mol Cell Biol*. 2002;22:1184–1193.
33. Hao YH, Lafita-Navarro MC, Zacharias L, et al. Induction of LEF1 by MYC activates the WNT pathway and maintains cell proliferation. *Cell Commun Signal*. 2019;17:129.
34. Martin K, Reimann A, Fritz RD, Ryu H, Jeon NL, Pertz O. Spatio-temporal co-ordination of RhoA, Rac1 and Cdc42 activation during prototypical edge protrusion and retraction dynamics. *Sci Rep*. 2016;6:21901.
35. Rao PV, Peterson YK, Inoue T, Casey PJ. Effects of pharmacologic inhibition of protein geranylgeranyltransferase type I on aqueous humor outflow through the trabecular meshwork. *Invest Ophthalmol Vis Sci*. 2008;49:2464–2471.
36. Pattabiraman PP, Rinkoski T, Poeschla E, Proia A, Challa P, Rao PV. RhoA GTPase-induced ocular hypertension in a rodent model is associated with increased fibrogenic activity in the trabecular meshwork. *Am J Pathol*. 2015;185:496–512.
37. Takahashi H, Noda S, Mashima Y, et al. The myocilin (MYOC) gene expression in the human trabecular meshwork. *Curr Eye Res*. 2000;20:81–84.
38. Kokotas H, Kroupis C, Chiras D, et al. Biomarkers in primary open angle glaucoma. *Clin Chem Lab Med*. 2012;50:2107–2119.
39. Clevers H, Nusse R. Wnt/beta-catenin signaling and disease. *Cell*. 2012;149:1192–1205.
40. Liu C, Li Y, Semenov M, et al. Control of beta-catenin phosphorylation/degradation by a dual-kinase mechanism. *Cell*. 2002;108:837–847.
41. Maher MT, Mo R, Flozak AS, Peled ON, Gottardi CJ. Beta-catenin phosphorylated at serine 45 is spatially uncoupled from beta-catenin phosphorylated in the GSK3 domain: implications for signaling. *PLoS One*. 2010;5:e10184.
42. Yan D, Wiesmann M, Rohan M, et al. Elevated expression of axin2 and hnkd mRNA provides evidence that Wnt/beta -catenin signaling is activated in human colon tumors. *Proc Natl Acad Sci U S A*. 2001;98:14973–14978.
43. Endo M, Nishita M, Minami Y. Analysis of Wnt/planar cell polarity pathway in cultured cells. *Methods Mol Biol*. 2012;839:201–214.
44. Rodrigues P, Macaya I, Bazzocco S, et al. RHOA inactivation enhances Wnt signalling and promotes colorectal cancer. *Nat Commun*. 2014;5:5458.
45. Lumetti S, Mazzotta S, Ferrillo S, et al. RhoA controls Wnt upregulation on microstructured titanium surfaces. *Biomed Res Int*. 2014;2014:401859.
46. Yuan Y, Call MK, Yuan Y, et al. Dexamethasone induces cross-linked actin networks in trabecular meshwork cells through noncanonical wnt signaling. *Invest Ophthalmol Vis Sci*. 2013;54:6502–6509.
47. Hoare MJ, Grierson I, Brotchie D, Pollock N, Cracknell K, Clark AF. Cross-linked actin networks (CLANs) in the trabecular meshwork of the normal and glaucomatous human eye in situ. *Invest Ophthalmol Vis Sci*. 2009;50:1255–1263.
48. Clark AF, Brotchie D, Read AT, et al. Dexamethasone alters F-actin architecture and promotes cross-linked actin network formation in human trabecular meshwork tissue. *Cell Motil Cytoskeleton*. 2005;60:83–95.
49. Clark AF, Wordinger RJ. The role of steroids in outflow resistance. *Exp Eye Res*. 2009;88:752–759.


Investigative Ophthalmology & Visual Science

50. Montecchi-Palmer M, Bermudez JY, Webber HC, Patel GC, Clark AF, Mao W. TGFbeta2 induces the formation of cross-linked actin networks (CLANs) in human trabecular meshwork cells through the Smad and Non-Smad dependent pathways. *Invest Ophthalmol Vis Sci*. 2017;58:1288–1295.
51. Bermudez JY, Montecchi-Palmer M, Mao W, Clark AF. Cross-linked actin networks (CLANs) in glaucoma. *Exp Eye Res*. 2017;159:16–22.
52. Clark R, Nosie A, Walker T, et al. Comparative genomic and proteomic analysis of cytoskeletal changes in dexamethasone-treated trabecular meshwork cells. *Mol Cell Proteomics*. 2013;12:194–206.
53. Filla MS, Woods A, Kaufman PL, Peters DM. Beta1 and beta3 integrins cooperate to induce syndecan-4-containing cross-linked actin networks in human trabecular meshwork cells. *Invest Ophthalmol Vis Sci*. 2006;47:1956–1967.
54. Clark AF, Wilson K, McCartney MD, Miggans ST, Kunkle M, Howe W. Glucocorticoid-induced formation of cross-linked actin networks in cultured human trabecular meshwork cells. *Invest Ophthalmol Vis Sci*. 1994;35:281–294.
55. Matsumoto Y, Johnson DH. Dexamethasone decreases phagocytosis by human trabecular meshwork cells in situ. *Invest Ophthalmol Vis Sci*. 1997;38:1902–1907.
56. Zhang X, Ognibene CM, Clark AF, Yorio T. Dexamethasone inhibition of trabecular meshwork cell phagocytosis and its modulation by glucocorticoid receptor beta. *Exp Eye Res*. 2007;84:275–284.
57. Webber HC, Bermudez JY, Millar JC, Mao W, Clark AF. The role of Wnt/beta-catenin signaling and K-cadherin in the regulation of intraocular pressure. *Invest Ophthalmol Vis Sci*. 2018;59:1454–1466.
58. Stumpff F, Wiederholt M. Regulation of trabecular meshwork contractility. *Ophthalmologica*. 2000;214:33–53.
59. Melendez J, Liu M, Sampson L, et al. Cdc42 coordinates proliferation, polarity, migration, and differentiation of small intestinal epithelial cells in mice. *Gastroenterology*. 2013;145:808–819.
60. Hanna SJ, McCoy-Simandle K, Miskolci V, et al. The role of Rho-GTPases and actin polymerization during macrophage tunneling nanotube biogenesis. *Sci Rep*. 2017;7:8547.
61. Keller KE, Bradley JM, Sun YY, Yang YF, Acott TS. Tunneling nanotubes are novel cellular structures that communicate signals between trabecular meshwork cells. *Invest Ophthalmol Vis Sci*. 2017;58:5298–5307.
62. Halder G, Dupont S, Piccolo S. Transduction of mechanical and cytoskeletal cues by YAP and TAZ. *Nat Rev Mol Cell Biol*. 2012;13:591–600.
63. Schroeder MC, Halder G. Regulation of the Hippo pathway by cell architecture and mechanical signals. *Semin Cell Dev Biol*. 2012;23:803–811.
64. Dupont S, Morsut L, Aragona M, et al. Role of YAP/TAZ in mechanotransduction. *Nature*. 2011;474:179–183.
65. Zemke NR, Gou D, Berk AJ. Dedifferentiation by adenovirus E1A due to inactivation of Hippo pathway effectors YAP and TAZ. *Genes Dev*. 2019;33:828–843.
66. Lee JY, Chang JK, Dominguez AA, et al. YAP-independent mechanotransduction drives breast cancer progression. *Nat Commun*. 2019;10:1848.
67. Tripathi RC, Li J, Chan WF, Tripathi BJ. Aqueous humor in glaucomatous eyes contains an increased level of TGF-beta 2. *Exp Eye Res*. 1994;59:723–727.
68. Kottler UB, Junemann AG, Aigner T, Zenkel M, Rummelt C, Schlotzer-Schrehardt U. Comparative effects of TGF-beta 1 and TGF-beta 2 on extracellular matrix production, proliferation, migration, and collagen contraction of human Tenon's capsule fibroblasts in pseudoexfoliation and primary open-angle glaucoma. *Exp Eye Res*. 2005;80:121–134.
69. Junglas B, Kuespert S, Seleem AA, et al. Connective tissue growth factor causes glaucoma by modifying the actin cytoskeleton of the trabecular meshwork. *Am J Pathol*. 2012;180:2386–2403.
70. Taylor AW. Primary open-angle glaucoma: a transforming growth factor-beta pathway-mediated disease. *Am J Pathol*. 2012;180:2201–2204.
71. Raghunathan VK, Thomasy SM, Strom P, et al. Tissue and cellular biomechanics during corneal wound injury and repair. *Acta Biomater*. 2017;58:291–301.
72. Overby DR, Zhou EH, Vargas-Pinto R, et al. Altered mechanobiology of Schlemm's canal endothelial cells in glaucoma. *Proc Natl Acad Sci U S A*. 2014;111:13876–13881.
73. Yan Q, Sage EH. SPARC, a matricellular glycoprotein with important biological functions. *J Histochem Cytochem*. 1999;47:1495–1506.
74. Brekken RA, Sage EH. SPARC, a matricellular protein: at the crossroads of cell-matrix communication. *Matrix Biol*. 2001;19:816–827.
75. Oh DJ, Kang MH, Ooi YH, Choi KR, Sage EH, Rhee DJ. Overexpression of SPARC in human trabecular meshwork increases intraocular pressure and alters extracellular matrix. *Invest Ophthalmol Vis Sci*. 2013;54:3309–3319.
76. Kuespert S, Junglas B, Braunger BM, Tamm ER, Fuchshofer R. The regulation of connective tissue growth factor expression influences the viability of human trabecular meshwork cells. *J Cell Mol Med*. 2015;19:1010–1020.
77. Suzuki Y, Shirato S, Taniguchi F, Ohara K, Nishimaki K, Ohta S. Mutations in the TIGR gene in familial primary open-angle glaucoma in Japan. *Am J Hum Genet*. 1997;61:1202–1204.
78. Tamm ER, Russell P, Epstein DL, Johnson DH, Piatigorsky J. Modulation of myocilin/TIGR expression in human trabecular meshwork. *Invest Ophthalmol Vis Sci*. 1999;40:2577–2582.
79. Fautsch MP, Bahler CK, Jewison DJ, Johnson DH. Recombinant TIGR/MYOC increases outflow resistance in the human anterior segment. *Invest Ophthalmol Vis Sci*. 2000;41:4163–4168.
80. Kasetti RB, Phan TN, Millar JC, Zode GS. Expression of mutant myocilin induces abnormal intracellular accumulation of selected extracellular matrix proteins in the trabecular meshwork. *Invest Ophthalmol Vis Sci*. 2016;57:6058–6069.
81. Cox TR, Erler JT. Remodeling and homeostasis of the extracellular matrix: implications for fibrotic diseases and cancer. *Dis Model Mech*. 2011;4:165–178.
82. Kagan HM, Li W. Lysyl oxidase: properties, specificity, and biological roles inside and outside of the cell. *J Cell Biochem*. 2003;88:660–672.
83. Sethi A, Wordinger RJ, Clark AF. Focus on molecules: lysyl oxidase. *Exp Eye Res*. 2012;104:97–98.
84. Beninati S, Piacentini M. The transglutaminase family: an overview: minireview article. *Amino Acids*. 2004;26:367–372.
85. Greenberg CS, Birckbichler PJ, Rice RH. Transglutaminases: multifunctional cross-linking enzymes that stabilize tissues. *FASEB J*. 1991;5:3071–3077.
86. Tovar-Vidales T, Clark AF, Wordinger RJ. Focus on molecules: transglutaminase 2. *Exp Eye Res*. 2011;93:2–3.
87. Levental KR, Yu H, Kass L, et al. Matrix crosslinking forces tumor progression by enhancing integrin signaling. *Cell*. 2009;139:891–906.


Investigative Ophthalmology & Visual Science

88. Raychaudhuri U, Millar JC, Clark AF. Tissue transglutaminase elevates intraocular pressure in mice. *Invest Ophthalmol Vis Sci*. 2017;58:6197–6211.
89. Raychaudhuri U, Millar JC, Clark AF. Knockout of tissue transglutaminase ameliorates TGFbeta2-induced ocular hypertension: a novel therapeutic target for glaucoma? *Exp Eye Res*. 2018;171:106–110.
90. Keller KE, Aga M, Bradley JM, Kelley MJ, Acott TS. Extracellular matrix turnover and outflow resistance. *Exp Eye Res*. 2009;88:676–682.
91. Keller KE, Acott TS. The juxtacanalicular region of ocular trabecular meshwork: a tissue with a unique extracellular matrix and specialized function. *J Ocul Biol*. 2013;1:3.

Investigative Ophthalmology & Visual Science